Ultrafast Excited-State Dynamics and Vibrational Cooling of 8-oxo-7,8-dihydro-2'deoxyguanosine in D_2O

Supporting Information

Yuyuan Zhang,[1] Jordon Dood,[1] Ashley Beckstead,[1] Jinquan Chen,[1,#] Xi-Bo Li,[2] Cynthia J. Burrows,[2] Zhen Lu,[3] Spiridoula Matsika,[3] and Bern Kohler[1,*]

[1] Department of Chemistry and Biochemistry, Montana State University, Bozeman, Montana 59717, USA

[2] Department of Chemistry, University of Utah, 315 S. 1400 East, Salt Lake City, Utah 84112, USA

[3] Department of Chemistry, Temple University, Philadelphia, Pennsylvania, 19122, USA

[#] Current Address: Department of Chemistry, Emory University, Atlanta, Georgia 30322, USA

* Corresponding Author:

Bern Kohler: kohler@chemistry.montana.edu, Tel: +1 406-994-7931, Fax: +1 406-994-5407

1. Exponential Fits to Kinetics at Selected Probe Frequencies

In the UV-pump/broadband-mid-IR-probe experiments, the solute kinetics at $t < 1$ ps are uncertain due to overlapping free induction decay and coherent artifacts.[1] Therefore, subpicosecond time constants are not reported.

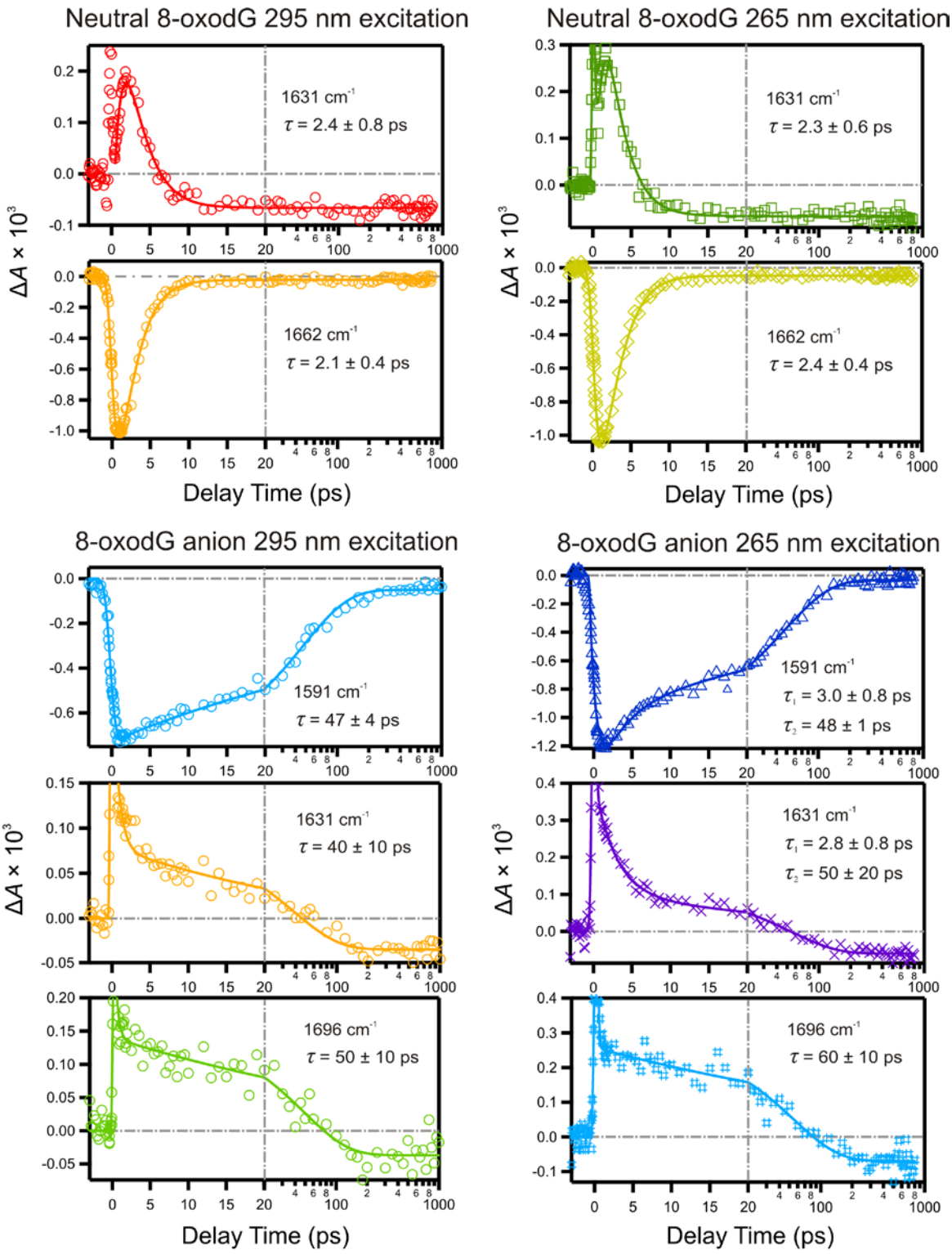

Figure S1. Exponential fits to kinetics at selected probe frequencies in the UV-pump/broadband-mid-IR-probe experiments.

For the neutral form, the bleach recovery signal at 1662 cm^{-1} was fitted to a bi-exponential decay with a constant offset at long delay times. For the decay of the positive feature at 1631 cm^{-1}, a delta function is included to fit the "spike" around t = 0 ps due to the instrument response. A rise time shorter than 1 ps is needed to fit the early time kinetics. For the anion, the bleach recovery following 295 nm excitation was fitted to a bi-exponential decay, but the fast component with positive amplitude was shorter than 1 ps. For the positive features at 1631 and 1696 cm^{-1}, a delta function was again included to fit the instrument response, and a fast time constant shorter than 1 ps was again found. The bleach recovery following 265 nm excitation was fitted to a tri-exponential decay, but the fastest component has a positive amplitude and time constant shorter than 1 ps. The signal at 1631 cm^{-1} was also fitted to a tri-exponential decay with a τ < 1 ps component. The 1696 cm^{-1} kinetics, however, was well described by a single exponential decay with a delta function.

2. Comparison of Bleach Recovery Kinetics

The red and green traces displayed in Figure S2 are identical to the experimental data shown in Figures 3a and 3b in the main text, respectively. These traces show the kinetics for neutral 8-oxodG at 1662 cm^{-1} obtained by UV-pump (295 nm and 265 nm) and broadband mid-IR probe. They overlap almost perfectly, even though the fits yield slightly different time constants. The blue trace (267 nm pump, 250 nm probe) monitors the bleach recovery of the electronic transition. The fitting produces a bleach recovery time that is very similar to those obtained from monitoring the ground state vibrational modes in the fingerprint region (compare the blue trace to the red and green traces in Figure S2). It is important to note that the broadband mid-IR probing experiments were performed with 10 mM of 8-oxodG in D_2O buffer solution, whereas

the 250 nm probing experiment was obtained from 1 mM of 8-oxodG. The consistency between the low and high concentration kinetics, and the absence of TA signals at long delay time (see main text), suggests that the 8-oxodG monomer does not form higher-order structures (aggregates due to stacking and/or base pairing) at high concentrations.

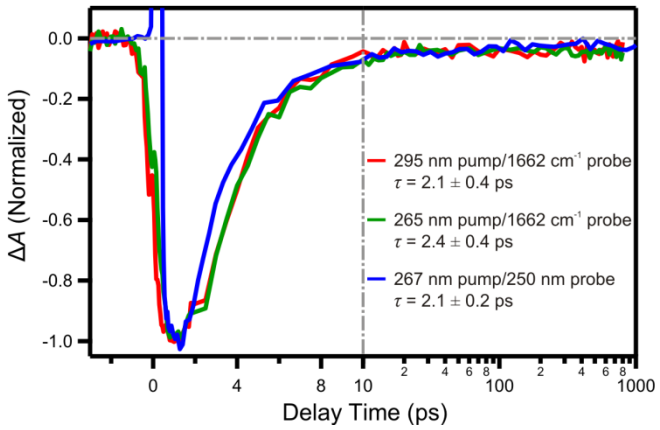

Figure S2. Comparison of the ground state bleach recovery kinetics for neutral 8-oxodG upon 295 vs. 265 nm excitation (compare red and green traces), and comparison of the ground state bleach recovery time between mid-IR probe and 250 nm probe (green and blue traces).

3. Correction Procedure for Removing Solvated Electron Signals

The procedure for removing the contribution to a TA signal from solvated electrons produced by two-photon ionization of the solvent has been described previously.[2,3] Briefly, an AMP solution (with the same concentration of phosphate buffer and NaCl) was prepared that has identical absorbance at 267 nm as the solution under investigation, either neutral 8-oxodG or its anion (vide infra). The pD of the AMP solution was adjusted to be identical to the corresponding 8-oxodG solution (pD 7.0 or 10.4). Because photoexcitation of AMP by 267 nm (4.65 eV) does not lead to any long-lived state, the TA signals from the AMP solution at $t > 2$ ps originate solely from solvated electrons generated by two-photon ionization of the solvent. The same amount of solvated electrons is generated in the 8-oxodG solution because the 8-oxodG and AMP solutions

have identical one-photon absorbance. The TA signal recorded separately from a buffer-only solution was then scaled to "tail match" the AMP signal, and subsequently subtracted from the 8-oxodG TA signal. Back-to-back TA measurements on 8-oxodG, AMP and the buffer-only solution (50 mM phosphate buffer and 100 mM NaCl in D_2O) were carried out under the same experimental conditions, ensuring that the pump fluence is identical for each experiment. The individual transients used in the correction procedure are shown in panels a and c of Figure S3 for the neutral and basic experiments, respectively. The final corrected transients are shown in panels b and d of Figure S3.

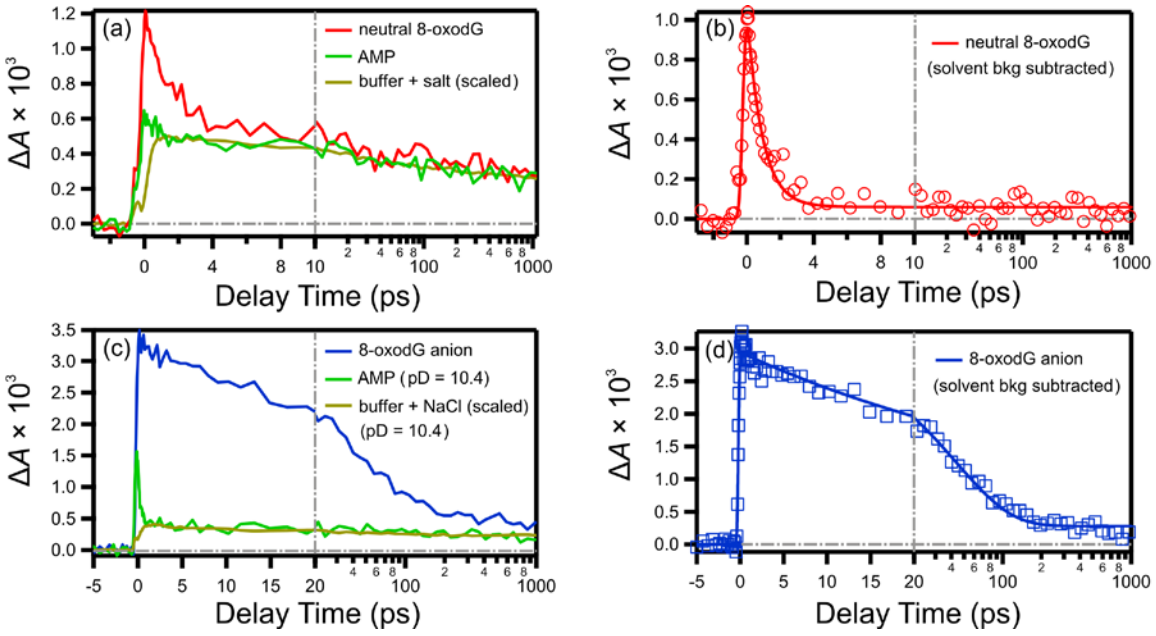

Figure S3. Kinetic traces obtained from sequential 267 nm pump / 570 nm probe experiments of 8-oxodG, AMP and buffer solutions under the same experimental conditions (0.9 μJ pump energy, 220 μm fwhm pump spot size). (a) Neutral 8-oxodG before subtraction, (b) after subtraction; (c) 8-oxodG anion before subtraction, (d) after subtraction.

Figure S4 shows a fit to the uncorrected TA signal (267 nm pump, 570 nm probe) for 8-oxodG at neutral pD using the sum of three exponentials. The shortest time constant of 0.9 ± 0.4

ps is in excellent agreement with the fast decay in the corrected transient (Figure S3b). The two longer time constants (13 ± 9 ps, 3 ± 2 ns) agree well with a biexponential fit to the buffer-only TA signal at times longer than 2 ps. This phenomenological fit (the actual decay of the solvated electron signal reflects more complex geminate recombination dynamics) supports the conclusion that the neutral 8-oxodG signal at times greater than 5 ps arises solely from solvated electrons.

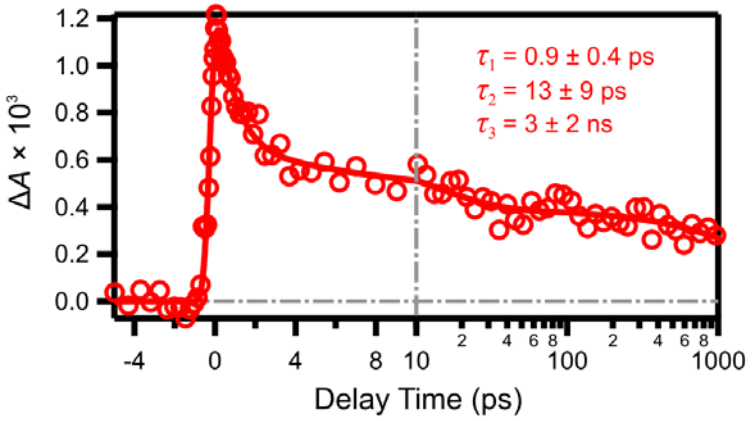

Figure S4. Uncorrected transient absorption signal (267 nm pump, 570 nm probe) for neutral 8-oxodG (red circles, same as red trace in Figure S3) along with a fit to three exponentials.

4. Determination of the Triplet Yield of 8-oxodG by the Eu^{3+} Energy Transfer Method

The intersystem crossing (ISC) quantum yield for 8-oxodG was measured using Eu^{3+} as an energy acceptor, following a procedure first described by Lamola and Eisinger.[4,5] Eu^{3+} has low-lying triplet states, which are able to accept energy from either the singlet or triplet states of a donor molecule. This lanthanide ion is well suited to quantifying ISC yields of DNA/RNA bases because its extinction coefficient in the deep-UV region is on the order of just 1 M^{-1} cm^{-1},[6] or 3 to 4 orders of magnitude lower than the nucleobases. In this case, UV excitation selectively

excites the bases. Acetophenone, a ketone with unit ISC quantum yield, was used as a standard. Acetophenone was dissolved in D_2O containing various concentrations of europium chloride. Using a bench-top steady-state fluorometer, the solution was excited at 267 nm in a 1 cm path length fused silica cell, and Eu^{3+} emission spectra were recorded from 550 to 750 nm.

The inverse of the emission intensity at 697 nm ($1/I_{fluo}$) was plotted against the inverse Eu^{3+} concentration ($1/[Eu^{3+}]$) and fitted to a line. The same procedure was then followed for D_2O solutions of neutral 8-oxodG. The ratio of the y-intercept for acetophenone to that measured for 8-oxodG is equal to the ISC quantum yield of 8-oxodG divided by the ISC yield for acetophenone (assumed to be equal to unity). The kinetic model that underlies this procedure has been described more thoroughly elsewhere.[4,5] It is important to point out that Eu^{3+} can act as a singlet energy acceptor when its concentration is high enough (e.g. > 20 mM for some DNA bases).[5] For this reason, the concentration of Eu^{3+} in our measurements was kept below 7 mM.

The ISC quantum yield for 8-oxodG was determined to be 0.06 ± 0.03% (the large standard deviation is due to the small emission counts). To test the accuracy of our measurements, the same protocol was carried out for thymine 5'-mononucleotide (TMP). Our result for the triplet quantum yield of TMP of 0.60 ± 0.06% is in excellent agreement with the value reported in ref. 5 (0.8%).[5] Thus, we can safely conclude that the ISC yield for 8-oxodG is less than that of TMP but possibly similar to the ISC yield for GMP (0.04%).[5] We were unable to estimate the ISC quantum yield for the anionic form of 8-oxodG because europium oxide precipitates under basic conditions.

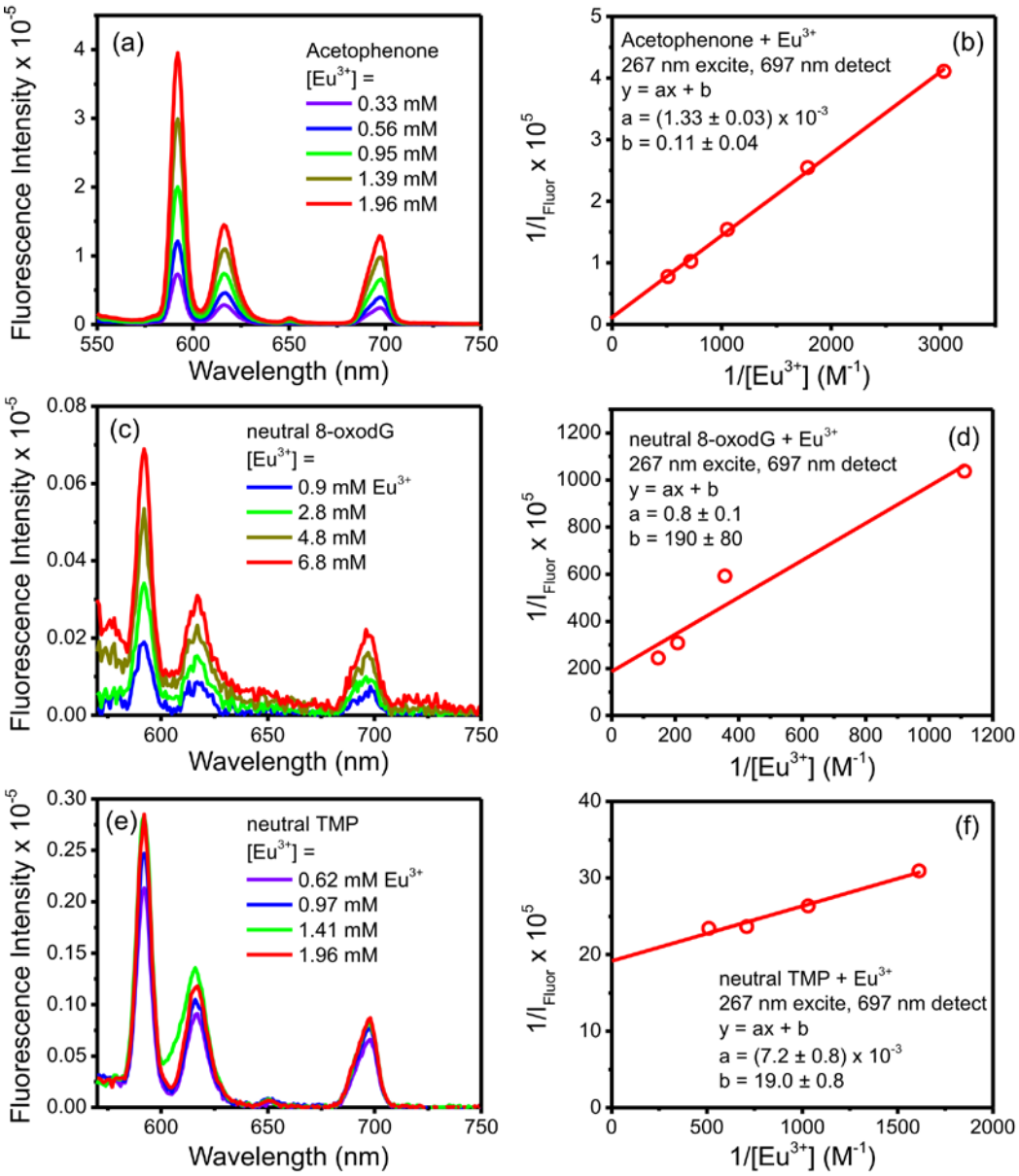

Figure S5. Eu^{3+} as a triplet energy acceptor for excited state acetophenone (a, b), neutral 8-oxodG (c, d) and TMP (e, f). The inverse of the emission intensity at 697 nm is plotted against the inverse of Eu^{3+} concentration (b, d, f), and the relative ratio between the y-intercepts gives the relative ISC quantum yield.

5. Theoretical Methods and Results

5.1 Methods

The geometries of neutral 8-oxoguanine and its deprotonated form were optimized at the MP2/6-31G(d) level. The geometries are almost planar except for a pyramidalization of the amino group. The excitation energies were computed using multi-configurational quasi-degenerate perturbation theory (MCQDPT2) and the cc-pvdz basis set with a (22, 15) active space. The orbitals in the active space were all the 12 π orbitals and 3 lone pairs. Initially, a CASSCF with an average of 4 states in each symmetry (A' and A'') was used, followed by MCQDPT2 to include dynamical correlation. The GAMESS software[7] was used for these calculations. For the excited state calculations, the molecules were restricted to planar symmetry, as Cs symmetry is less expensive computationally. The effect of this restriction on the excited states is ~0.1 eV. The basis set used for the excited states at the MCQDPT2 level does not include any diffuse functions, and thus πσ* states are not computed. Because the vertical detachment energy (VDE, energy to remove the least bound electron) in the gas phase is below the excited states, inclusion of diffuse functions creates an increased number of πσ* states (attempting to create a continuum of the removed electron). In order to avoid this problem we have not used diffuse basis functions.

The VDE from the deprotonated form was calculated using the EOM-IP-CCSD/6-31+G(d) method and the QChem computational package.[8] In order to include the solvation in the calculation of VDE the polarizable continuum model (PCM) was included in the EOM-IP-CCSD calculation. Specifically, the surface and simulation of volume polarization for electrostatics (SSVPE) approach[9] as implemented in QChem was used.

5.2 Excited State Energies

The vertical excitation energies of neutral and deprotonated 8-oxoguanine at the MCQDPT2/cc-pvdz level are summarized in Table S1. The energies of guanine are also included (data taken from ref. 10) and they are in good agreement with energies calculated at the CASPT2 level.[11] The three lowest energy transitions of all systems consist of two ππ* (L_a, L_b) states and an nπ* state. The transition energies for the ππ* states are in reasonable agreement with the experimental absorption maxima (see Table S1 and Figure 1a in the main text). The energies of the first π*←π transition is overestimated by 0.01 – 0.22 eV, while the second π*←π transition is overestimated by 0.05 – 0.5 eV. However, the trends between molecules are well reproduced. 8-oxoguanine is predicted to have absorption peaks that are red-shifted compared to guanine while deprotonation of 8-oxoguanine leads to a red-shifted first ππ* state and a blue-shifted second ππ* state.

Table S1. Calculated and experimental vertical transition energies for the three lowest excited state of guanine, 8-oxoguanine and deprotonated 8-oxoguanine. The experimental values are the observed peak maxima for GMP and 8-oxodG (see Figure 1a in the main text).

	MCQDPT2 (eV)		expt. (eV)
Guanine	4.60	ππ*	4.58
	5.37	ππ*	4.92
	5.47	nπ*	
8-oxoguanine			
	4.45	ππ*	4.22
	5.59	ππ*	5.02
	5.69	nπ*	
deprotonated			
	4.62	ππ*	4.43
	4.88	nπ*	
	5.08	ππ*	5.02

The other predicted result that could be of importance to the excited state dynamics is that, for both neutral species, the nπ* state has higher energy than the two bright states, but for the deprotonated 8-oxoguanine it is between the two bright states. The energy of the nπ* state, however, is expected to be shifted in aqueous solution. In order to estimate this shift we calculated the excitation energies using TD-DFT and a simple polarizable solvation model. The results suggest that the nπ* state will be blue-shifted by ~0.3 eV in solution, which will place it above the bright states but not too far separated. Therefore, it is possible that very soon after absorption the dark state becomes involved in the dynamics. Further calculations beyond the Franck-Condon region are needed to better understand the interaction between the states and the ensuing dynamics.

5.3 Vertical Detachment Energy

The vertical detachment energy for the 8-oxoguanine anion is calculated to be 3.2 eV for the isolated molecule, and 6.9 eV in aqueous solution. Based on these VDE values, the excited states of the deprotonated form in the gas phase are resonances, embedded in the continuum. In aqueous solution, however, the lowest excited states should be bound.

References

1. Schrader, T.; Sieg, A.; Koller, F.; Schreier, W.; An, Q.; Zinth, W.; Gilch, P., Vibrational Relaxation Following Ultrafast Internal Conversion: Comparing IR and Raman Probing. *Chem. Phys. Lett.* **2004,** 392, 358-364.

2. Crespo-Hernández, C. E.; Kohler, B., Influence of Secondary Structure on Electronic Energy Relaxation in Adenine Homopolymers. *J. Phys. Chem. B* **2004,** 108, 11182-11188.

3. Chen, J. Q.; Kohler, B., Ultrafast Nonradiative Decay by Hypoxanthine and Several Methylxanthines in Aqueous and Acetonitrile Solution. *Phys. Chem. Chem. Phys.* **2012,** 14, 10677-10682.

4. Eisinger, J.; Lamola, A. A., Europium Ions as Probes for Excited Molecules in Aqueous Solution. *Biochim. Biophys. Acta* **1971,** 240, 299-312.

5. Lamola, A. A.; Eisinger, J., Excited States of Nucleotides in Water at Room Temperature. *Biochim. Biophys. Acta* **1971,** 240, 313-325.

6. Gallagher, P. K., Absorption and Fluorescence of Europium(III) in Aqueous Solutions. *J. Chem. Phys.* **1964,** 41, 3061-3069.

7. Schmidt, M. W.; Baldridge, K. K.; Boatz, J. A.; Elbert, S. T.; Gordon, M. S.; Jensen, J. H.; Koseki, S.; Matsunaga, N.; Nguyen, K. A.; Su, S. J., *et al.*, General Atomic and Molecular Electronic-Structure System. *J. Comput. Chem.* **1993,** 14, 1347-1363.

8. Shao, Y.; Molnar, L. F.; Jung, Y.; Kussmann, J.; Ochsenfeld, C.; Brown, S. T.; Gilbert, A. T. B.; Slipchenko, L. V.; Levchenko, S. V.; O'Neill, D. P., *et al.*, Advances in Methods and Algorithms in a Modern Quantum Chemistry Program Package. *Phys. Chem. Chem. Phys.* **2006,** 8, 3172-3191.

9. Chipman, D. M., Reaction Field Treatment of Charge Penetration. *J. Chem. Phys.* **2000,** 112, 5558-5565.

10. Mburu, E.; Matsika, S., An Ab Initio Study of Substituent Effects on the Excited States of Purine Derivatives. *J. Phys. Chem. A* **2008,** 112, 12485-12491.

11. Barbatti, M.; Szymczak, J. J.; Aquino, A. J. A.; Nachtigallova, D.; Lischka, H., The Decay Mechanism of Photoexcited Guanine - a Nonadiabatic Dynamics Study. *J. Chem. Phys.* **2011,** 134.